Near Real-Time Disturbance Detection Using Satellite Image Time Series: Drought Detection in Somalia

Jan Verbesselt
Wageningen University

Achim Zeileis
Universität Innsbruck

Martin Herold
Wageningen University

Abstract

Near real-time monitoring of ecosystem disturbances is critical for rapidly assessing and addressing impacts on carbon dynamics, biodiversity, and socio-ecological processes. Satellite remote sensing enables cost-effective and accurate monitoring at frequent time steps over large areas. Yet, generic methods to detect disturbances within newly captured satellite images are lacking. We propose a multi-purpose time-series-based disturbance detection approach that identifies and models stable historical variation to enable change detection within newly acquired data. Satellite image time series of vegetation greenness provide a global record of terrestrial vegetation productivity over the past decades. Here, we assess and demonstrate the method by applying it to (1) simulated time series of vegetation greenness data from satellite data, (2) real-world satellite greenness image time series between February 2000 and July 2011 covering Somalia to detect drought-related vegetation disturbances. First, simulation results illustrate that disturbances are successfully detected in near real-time while being robust to seasonality and noise. Second, major drought-related disturbance corresponding with most drought-stressed regions in Somalia are detected from mid-2010 onwards. The method can analyse in-situ or satellite data time series of biophysical indicators from local to global scale since it is fast, does not depend on thresholds and does not require time series gap filling. While the data and methods used are appropriate for proof-of-concept development of global scale disturbance monitoring, specific applications (e.g., drought or deforestation monitoring) mandates integration within an operational monitoring framework (e.g., http://www.fews.net/).

Keywords: early warning, real-time monitoring, global change, disturbance, time series, remote sensing, vegetation phenology, climate dynamics.

1. Introduction

Real-time disturbance detection is critical for signalling abnormal developments, quickly raising awareness and reducing negative impacts on natural resources, humans, and infrastructure. A disturbance can be defined as a relatively discrete event occurring over a short time period that disrupts the structure of an ecosystem, community, or population (Pickett and White 1986). Disturbances alter the system state and the trajectory of an ecosystem, and therefore are the key drivers of spatial and temporal heterogeneity (Turner 2010). Abiotic (e.g., fires, windstorms) and biotic (e.g., pest, pathogens) ecosystem disturbances can contribute to the

current rise of carbon dioxide (CO_2) levels in the atmosphere due to the emission of CO_2 from terrestrial biomass loss (Potter *et al.* 2003; Schimel *et al.* 2001).

Many recent disturbances occur worldwide at unknown locations. In this sense, remote sensing tools can be in the first instance used to alert for disturbances since satellite sensors are well-suited to provide consistent and frequent measurements over large areas. A common way to derive indicators of ecosystem dynamics is the use of spectral vegetation indices related to the photosynthetic capacity of vegetation canopies such as the Normalised Difference Vegetation Index (NDVI, Myneni *et al.* 1995; Pettorelli *et al.* 2005; Potter *et al.* 2003). Although NDVI might be affected by soil background and a saturation effect at high biomass levels, it captures seasonal and inter-annual changes in vegetation status (Huete *et al.* 2002; Myneni *et al.* 1997). Deviations from average season-trend vegetation dynamics over multiple years can indicate the effects of many processes that cause disturbances, including physical (e.g., droughts, fires, floods; Funk and Budde 2009; Vrieling *et al.* 2011), biogenic (e.g., herbivorous insects, pathogens; Hargrove *et al.* 2009; Stone *et al.* 2008; Verbesselt *et al.* 2009) and anthropogenic (e.g., deforestation, urbanisation; Asner 2011; Jin and Sader 2005; Potter *et al.* 2003). Ecosystem changes commonly observed with remote sensing approaches can be divided into three categories: (1) *seasonal or cyclic change*, for example driven by annual temperature and rainfall interactions impacting plant phenology resulting in distinct intra-annual patterns for different vegetation types; (2) *gradual trend change* such as trends in mean annual rainfall or gradual change in land management (e.g., long-term drought, forest regrowth after fire) that result in changes over several years; and (3) *abrupt trend change*, caused by events from human activities (e.g., deforestation) or natural causes (e.g., wind throw, or drought event) that change land surface over short time frames (e.g., days to weeks or months; Verbesselt *et al.* 2010a,b; Vogelmann *et al.* 2012). The detection of short-term abrupt changes (e.g., light frost, rainfall events) depends on the magnitude of change versus the signal-to-noise ratio often determined by the spectral, spatial and temporal characteristics of the remotely sensed data. This paper focuses on the detection of abrupt ecosystem changes further referred to as disturbances.

Detecting changes within time series is the first step towards understanding the acting processes and drivers (e.g., natural or anthropogenic). Estimating change from remotely sensed data series however is not straightforward, since time series contain a combination of seasonal, gradual and abrupt ecosystem changes occurring in parallel, in addition to noise that originates from the sensing environment (e.g., view angle), remnant geometric errors, atmospheric scatter and cloud effects (de Beurs and Henebry 2005; Roy *et al.* 2002; Wolfe *et al.* 1998). The ability of any system to detect ecosystem disturbances depends on its capacity to differentiate the normal phenological cycle from abnormal change. Several near real-time change detection methods utilising satellite data are available (Jiang *et al.* 2010; Verdin *et al.* 2005; White and Nemani 2006) but these methods can be improved upon by utilising the full temporal detail of the data time series. Three major challenges remain.

First, it is crucial to be able to detect disturbances within newly captured satellite images to enable a rapid response or early warning. In previous work, we proposed an approach, BFAST (Break detection For Additive Season and Trend), for change detection within seasonal time series (de Jong *et al.* 2011; Verbesselt *et al.* 2010a,b). BFAST detects and characterises trend and seasonal changes within historical time series but the method is not developed to detect disturbances in recently acquired data. Methods to detect changes in near real-time have been suggested in the statistics and econometrics literature to assess the stability of linear

regression models (Chu *et al.* 1996), e.g., for investigating exchange rate dynamics (Zeileis *et al.* 2010). However, these methods have not been optimised for real-time disturbance detection of terrestrial ecosystems using remotely sensed time series data.

Second, change detection techniques for global disturbance monitoring need to be independent of vegetation-specific thresholds while being robust against the inherent noise and seasonality captured within time series. Most change detection methods require user designation of a threshold or change type definition separating real change from spectral changes caused by variability in illumination, seasonality, or atmospheric scattering (Lu *et al.* 2004; Potter *et al.* 2003; Hayes and Cohen 2007). The determination of thresholds adds significant cost to efforts expanding change detection across regions or becomes complex when the regions are changing (White and Nemani 2006). A historical analysis using archived satellite data is needed to model normal, expected behaviour against which abnormal behaviour, i.e., disturbance, in the near future can be described (Hargrove *et al.* 2009). There is a critical need to enable analysis of time series independent of specific thresholds or definitions to detect disturbances.

Third, change detection methods need to deal with missing data (e.g., clouds or sensor defects) in time series data. Existing change detection methods smooth or fill gaps (Jönsson and Eklundh 2002; Roerink *et al.* 2000; Julien and Sobrino 2010) when dealing with noisy times series of remotely sensed data. For a given date, these methods typically require looking both backwards and forwards in time, negating use in real-time or forecast applications (White and Nemani 2006). Furthermore, gap filling techniques model data based on assumptions of normal data variation which inhibits the detection of disturbances (Samanta *et al.* 2011). Hence, methods able to analyse and detect changes in non-gap-filled time series are urgently needed for global change monitoring.

We propose a multi-purpose approach for near real-time disturbance detection using time series data that does not require specific thresholds and deals with missing data. The following major research questions are answered in this paper:

(1) Can a period, representing stable (i.e., normal) historical data variation representing both seasonal and gradual changes, be identified within a time series?

(2) Is the model representing a *normal* historical data variation able to reliably and quickly differentiate between normal and *abnormal* changes (i.e., disturbances) within newly incoming observations (i.e., near real-time)?

We assess this approach for different ecosystems by simulating NDVI time series with varying amounts of seasonal variation and noise, and by adding changes with different magnitudes representing a wide variety of terrestrial ecosystems. We demonstrate the proof of concept using the MODIS (Moderate Resolution Imaging Spectrometer) NDVI 16-day image composites from February 2000 until July 2011 for drought disturbance detection in Somalia. NDVI time series are also used by organisations like the Monitoring Agricultural Resources (MARS) unit at Joint Research Centre (JRC), the United States Famine Early Warning System Network (FEWS-NET), and the United Nations Food and Agricultural Organisation (FAO) as an early warning for potential food production problems in African countries (Rojas *et al.* 2005).

2. Material and methods

2.1. Real-time disturbance detection

While investigating ecosystem disturbances using satellite data, many approaches (e.g. Verbesselt *et al.* 2010b; White *et al.* 2009) focus on the question if and where disturbances occur in an observed time series $t = 1, \ldots, n$, we investigate a different question: *Do new observations $t = n, n+1, \ldots$ still conform with the expected behaviour of the historical sample $t = 1, \ldots, n$?* Thus, we are detecting disturbances at the end of a time series by comparison with representative, i.e., stable, historical observations. Here, a method is presented that is able to detect disturbances within newly acquired time series data by automatically identifying a stable history period (Section 2.4) to model the season-trend variation (Section 2.2) against which disturbances can be detected (Section 2.3).

Validation of multi-temporal change-detection methods is often not straightforward, since independent reference sources for a broad range of potential changes must be available (Kennedy *et al.* 2007). Thus, we simulated 16-day NDVI time series with different noise, seasonality, and disturbances levels in order to robustly test the disturbance detection approach in a controlled environment (Verbesselt *et al.* 2010a,b). However, it is challenging to create simulated time series that approximate remotely sensed time series, because these contain combined information on vegetation phenology, inter-annual climate variability, disturbance events, sensor conditions (e.g., viewing angle), and signal contamination (e.g., clouds) (Zhang *et al.* 2009). Hence, we tested the method by (1) a simulation experiment (Section 2.5) and (2) analysis of 16-day MODIS satellite NDVI time series for drought disturbance detection Somalia (Section 2.6).

2.2. Season-trend model

The method proposed here is based on a similar additive season and trend model as employed by Verbesselt *et al.* (2010b) to account for seasonal and trend changes typically occurring within climate-driven biophysical indicators derived from satellite data (e.g., NDVI) (de Beurs and Henebry 2005). For the observations y_t at time t, a season-trend model is assumed with linear trend and harmonic season:

$$y_t \;=\; \alpha_1 + \alpha_2 t + \sum_{j=1}^{k} \gamma_j \sin\left(\frac{2\pi j t}{f} + \delta_j\right) \;+\; \varepsilon_t, \tag{1}$$

where the intercept α_1, slope α_2 (i.e., trend), amplitudes $\gamma_1, \ldots, \gamma_k$, and phases $\delta_1, \ldots, \delta_k$ (i.e., season) are the unknown parameters, f is the known frequency (e.g., $f = 23$ annual observations for a 16-day time series), and ε_t is the unobservable error term at time t (with standard deviation σ). In the applications below, we employ three harmonic terms (i.e., $k = 3$) to robustly detect disturbances within MODIS NDVI time series, as components four and higher represent variations that occur on a three-month cycle or less (Geerken 2009; Julien and Sobrino 2010). The model (Equation 1) can be written as a standard linear regression model (see e.g. Cryer and Chan 2008, Chapter 3.3):

$$
\begin{aligned}
y_t \;&=\; x_t^\top \beta \;+\; \varepsilon_t, \\
x_t \;&=\; \{1, t, \sin(2\pi 1 t/f), \cos(2\pi 1 t/f), \ldots, \sin(2\pi k t/f), \cos(2\pi k t/f)\}^\top, \\
\beta \;&=\; \{\alpha_1, \alpha_2, \gamma_1 \cos(\delta_1), \gamma_1 \sin(\delta_1), \ldots, \gamma_k \cos(\delta_k), \gamma_k \sin(\delta_k)\}^\top,
\end{aligned}
$$

containing the $p = 2 + 2k$ regression parameters β which can be estimated and tested using ordinary least squares (OLS) techniques. If there are gaps in the time series y_t, these observations are simply omitted prior to estimation of β which can then still consistently be identified (unless *all* observations at certain frequencies are missing). The season-trend model takes the underlying trend and seasonal variation within a time series into account so that season-trend patterns are removed in the resulting residuals. This corresponds to approaches where in multiple steps a time series is 'detrended' and 'deseasonalized' (e.g. Potter *et al.* 2003), whereas here the adjustment is done in a single step by OLS fitting of the season-trend model. If no trend and/or nor seasonality are present in the data investigated, the corresponding elements of the regressor can also be omitted.

2.3. Monitoring structural change

Based on the season-trend model introduced above, the question raised in the introduction can be rephrased: *Given that a stable season-trend model was estimated in an observed time period, does it remain stable for new observations?* A disturbance is detected when the model does not remain stable for new incoming observations. As the season-trend model can be formulated as an OLS regression, we can leverage methods proposed in the structural change literature for linear regression models where this problem is known as *monitoring* of structural changes (Chu *et al.* 1996). The idea for monitoring techniques is simple. Given that the parameters β can be consistently estimated as $\hat{\beta}$ from a stable history period $t = 1, \ldots, n$, we want to check whether $\hat{\beta}$ still fits the data y_t for $t > n$ (i.e., for new data). To do so, some measure of discrepancy is needed (Chu *et al.* 1996; Leisch *et al.* 2000; Zeileis 2005). Here, we use moving sums (MOSUMs) of the residuals in the monitoring period $t = n + 1, \ldots, N$:

$$MO_t = \frac{1}{\hat{\sigma}\sqrt{n}} \sum_{s=t-h+1}^{t} (y_s - x_s^\top \hat{\beta}), \qquad (2)$$

where h is the bandwidth of the MOSUM and is typically chosen relative to the size of the history sample, e.g., $h = n/4$ or $h = n$ (Zeileis 2005; Zeileis *et al.* 2010). If the model remains stable, the MOSUM process MO_t should be close to zero and fluctuate only randomly. However, if a structural change occurs, MO_t will deviate systematically from zero. A structural break is declared if the absolute value $|MO_t|$ exceeds some boundary that is asymptotically only crossed with 5% probability under structural stability. If there are missing values in y_t in the monitoring period, these are again simply not included in the MOSUM MO_t, i.e., only reduce the number of observations available. The technical details for the boundary are based on a so called functional central limit theorem (see Leisch *et al.* 2000, for details). The boundary function employed here is taken from Zeileis *et al.* (2005, Equation 7).

2.4. Selecting the stable history period

A crucial assumption for the monitoring approach proposed above is that the history period $t = 1, \ldots, n$ itself is free of disturbances, so that the parameters β are stable during this time and can be used to model normal expected behaviour. In practice, there are often long series of observations y_t available before the start of the monitoring process and it would be naive to assume that always all of these observations can be adequately captured by a single season-trend model. Hence, a natural idea is to not use all observations but only the last $\ell, \ldots, n$
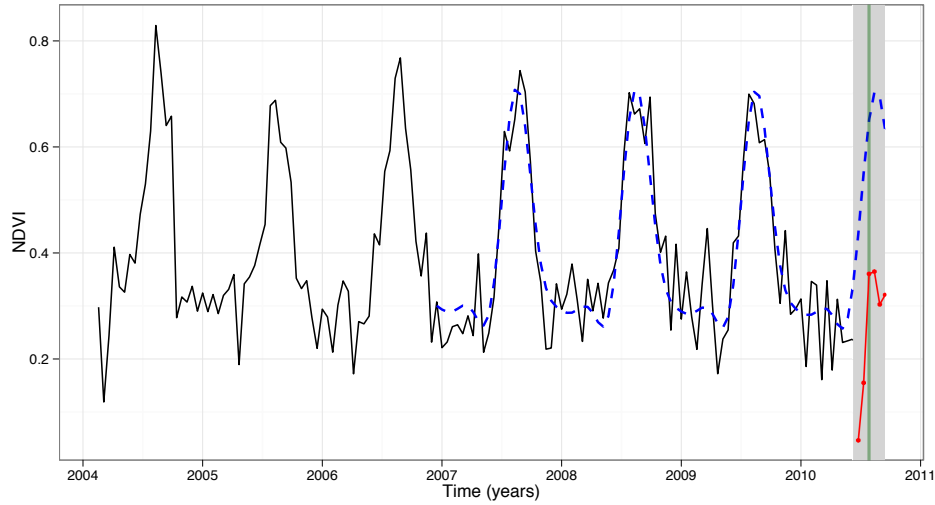
Figure 1: Simulated 16-day MODIS NDVI time series with $a = 0.4$, $\sigma = 0.05$, containing one simulated abrupt change with $m = -0.3$). The period from 2004 until mid-2010 (i.e., the time step just before the simulated break), is considered the *history period* and the period after the simulated break is the *monitoring period* (grey background). The monitoring period contains 6 observations ($d = 6$, red line). The result of the monitoring approach is shown: A stable history period is identified within the history period (i.e., 2007 until mid-2010) and used to model and predict the normal data variation (blue dashed line) to enable disturbance detection (Section 2.3). Here, a disturbance is detected after 3 observations in the monitoring period (green vertical line).

observations with $\ell \geq 1$ so that a stable season-trend model can be fitted. In principle, the start ℓ of the history period could be chosen based on expert knowledge but for automatic applications a data-driven choice is desirable. Here, we implement a technique proposed by Pesaran and Timmermann (2002) that by moving backward in time for $t = n, n-1, n-2, \ldots$ evaluates a cumulative prediction error until the season-trend model (Equation 1) breaks down. The method is also known as reversed-ordered-cumulative sum (CUSUM) of residuals, or ROC. The CUSUM test (see Zeileis *et al.* 2002, for more details) is based on similar ideas as the monitoring approach introduced above and the ROC method simply applies it in reverse ordering. Some alternatives for choosing ℓ are discussed in Section 4.

Figure 1 provides an overview of the three steps that are being performed when applying the real-time disturbance detection approach. Two periods are defined within a time series; (a) a *history period*, i.e., data that already has been acquired and which will be analysed for stability in order to model normal vegetation dynamics, and (b) a *monitoring period*, i.e., the period representing new data that recently has been captured that needs to be analysed for disturbances. The blue line in Figure 1 illustrates the fit of the season-trend model on the identified stable part of the history period of an example NDVI time series (Section 2.2). This season-trend fit is used to model the normal expected behaviour in the *history period* and as such detect abnormal data variations, disturbances, within the *monitoring period* (Section 2.3). Here, a disturbance is detected with only a short delay.

Parameters	Values
a	$0.1, 0.3, 0.5$
σ noise	$0.01, 0.02, \ldots, 0.15$
m	$0, -0.2, -0.4, \ldots, -0.8$
d	$1, 2, \ldots, 6$

Table 1: Parameter values for simulation of 16-day NDVI time series: Amplitude a, noise level σ, and magnitude m of shift, while varying the amount of data available in the monitoring period (d, 16-day time steps units) to quantify the detection delay.

2.5. Simulation experiment

The objective of the time series simulation experiment is to assess the *detection delay*, i.e., how much new data is required to detect a disturbance, while varying the amount of noise, seasonal amplitude, and the magnitude of the disturbance in the simulated time series. NDVI time series were simulated using a similar approach as proposed by Verbesselt *et al.* (2010b) representing a wide range of ecosystem dynamics. Simulated NDVI time series are generated by summing individually simulated season, trend, and noise components.

First, the seasonal component is created using an asymmetric Gaussian function with an amplitude (a) for each season. Second, a disturbance was added to the trend component (e.g., fire or drought) by combining a step function with a magnitude (m) and fixed gradient recovery phase. Third, the noise component was generated using a random number generator that follows a normal distribution $\mathcal{N}(0, \sigma)$. Vegetation-index-specific noise was generated by randomly replacing the white noise by noise with a value of -0.1, representing cloud contamination that often remains after atmospheric correction and cloud masking procedures (see Verbesselt *et al.* 2010b, for more details). Figure 1 shows a simulated 16-day MODIS NDVI time series with $a = 0.4$, $\sigma = 0.05$, containing one simulated abrupt change with $m = -0.3$.

In the simulation experiment the *history period* is defined as the period from 2004 until mid-2010 (i.e., the time step just before the simulated break), whereas the *monitoring period* is defined as the period from the simulated break onwards of which the length is gradually increased during the experiment (d) (Figure 1 and Table 1). We selected a range of a, σ, and m values for the simulation study to represent a large range of land cover types of different data quality while varying the amount of data, d, available in the monitoring period (Table 1). Thousand iterations of all the combinations of σ, a, d and m were performed to quantify the probability of detecting a disturbance in the monitoring period in relation to the number of time series observations in the monitoring period (d).

2.6. Drought disturbance detection in Somalia

The use of the real-time monitoring approach is demonstrated using the 16-day MODIS NDVI composites with a 0.05° spatial resolution (MOD13C1 collection 5). This product provides NDVI corrected for the effect of atmospheric gases, thin cirrus clouds and aerosols as a measure for global scale vegetation dynamics and disturbances (Huete *et al.* 2002). The MOD13C1 global satellite images were acquired from February 2000 to July 2011. The full satellite image time series (February 2000 to July 2011) were analysed for disturbances
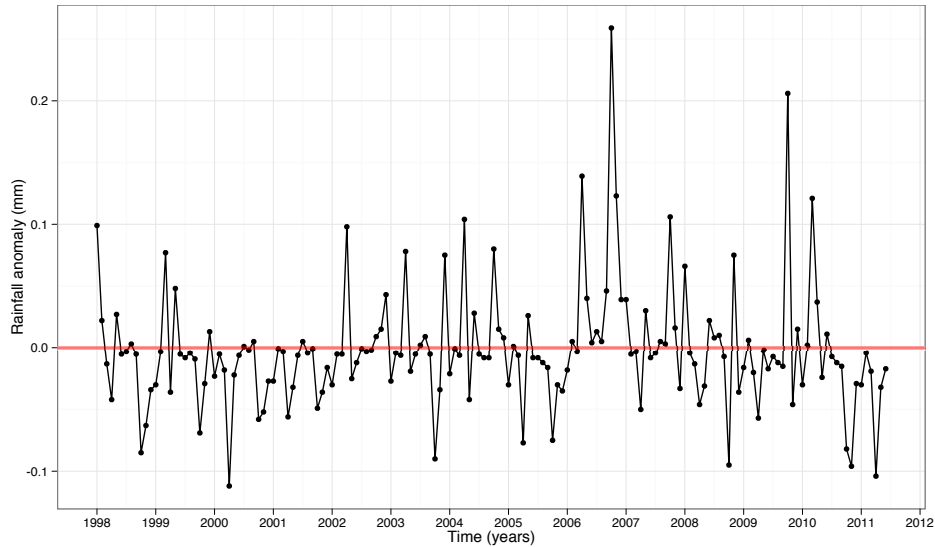
Figure 2: Monthly rainfall anomalies (mm) for the period 1998–2011 measured by the tropical rainfall measuring satellite mission (TRMM) for an area in South Somalia (2° Lat. and 43° Long.). The time series was derived from the TRMM 3B43 climatology (version 6) data set using the online visualisation and analysis system (TOVAS). Anomalies are computed as the difference between the measured precipitation and the average climatology for the selected region (Acker and Leptoukh 2007).

from mid-2010 onwards covering Somalia in order to assess the impact of the 2010–2011 drought on the vegetation photosynthetic capacity. The MODIS quality assurance (QA) flags are used to select only cloud-free data of optimal quality. An NDVI time series is only analysed when (1) less than 15% of observations masked out by the QA flags and (2) covering vegetated land; i.e., having a median of NDVI time series larger than 0.2 NDVI (de Beurs *et al.* 2009; de Jong *et al.* 2011; Vrieling *et al.* 2011). The noise level (σ) of NDVI time series is estimated by deriving the standard deviation of the residuals from the fitted season-trend model (Equation 1) on the stable history period. The magnitude and direction of the disturbance is estimated by deriving the difference between the median of the fitted season-trend model and the new observations during the monitoring period.

Study area

Somalia has a semi-arid tropical climate and there is little seasonal change in temperature. In the low areas, the mean temperature ranges from about 25° C to 28° C. Rain falls in two seasons of the year: heavy rains from March to May, and light rains from September to December. The annual rainfall is exceeding 500 mm only in Southern Somalia (Muchiri 2007). However, after a period of persistent poor rains during the past decade, the autumn 2010 rains were poor and the spring rains in 2011 failed completely (Funk 2011). The lack of rainfall combined with high food prices has weakened the population's resilience to food emergencies and are among the most important factors explaining the severe and ongoing famine in Somalia today. The monthly rainfall anomaly time series shown in Figure 2 illustrates the lack of rainfall in the last decade and the severity of the rainfall anomaly occurring from mid-2010
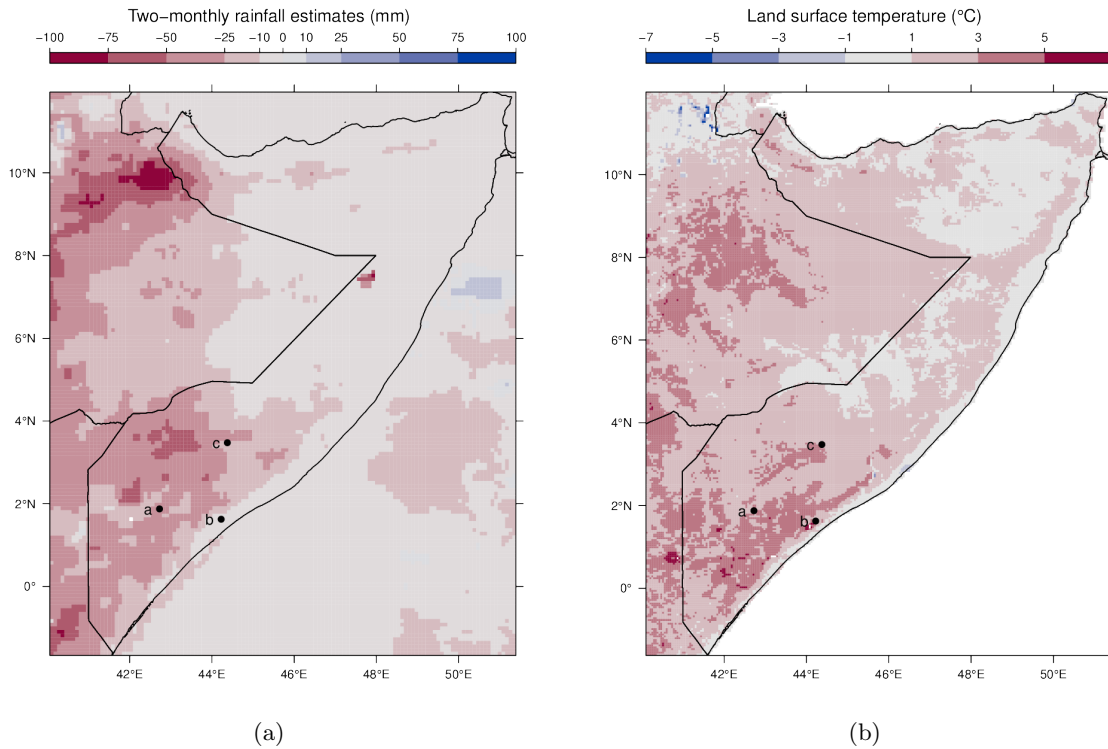
Figure 3: Anomaly in (a) two-monthly rainfall estimates (mm, RFE2) and (b) land surface temperature (°C, LST) for Somalia illustrating the below normal rainfall and above normal land surface temperature during the February-March period in 2011. The RFE2 data is a merged satellite-gauge rainfall product produced by NOAA's Climate Prediction Centre at a 0.1° spatial resolution. The LST product is the land surface temperature measured by the MODIS satellite and is provided at a 0.05° spatial resolution. Individual observations are subtracted from the time series mean to produce anomaly data. MODIS NDVI time series (2000–2011) for three locations (a, b, and c) are shown in Figure 6. The data were obtained using the Early Warning Explorer software tool available at http://earlywarning.usgs.gov/.

onwards in Southern Somalia. The spatial extent of the drought severity is illustrated by the February–March 2011 rainfall (Xie and Arkin 1997) and land surface temperature anomaly for Somalia (Figure 3). Below normal rainfall and above normal temperatures occurred during February–March 2011 in South Somalia.

3. Results

3.1. Simulation experiment

Figure 4 illustrates the probability for detecting a break within the monitoring period of a time series while varying the noise level (σ), magnitude of simulated disturbance (m) and the amount of data available in the monitoring period (d). The seasonal amplitude (a) did not
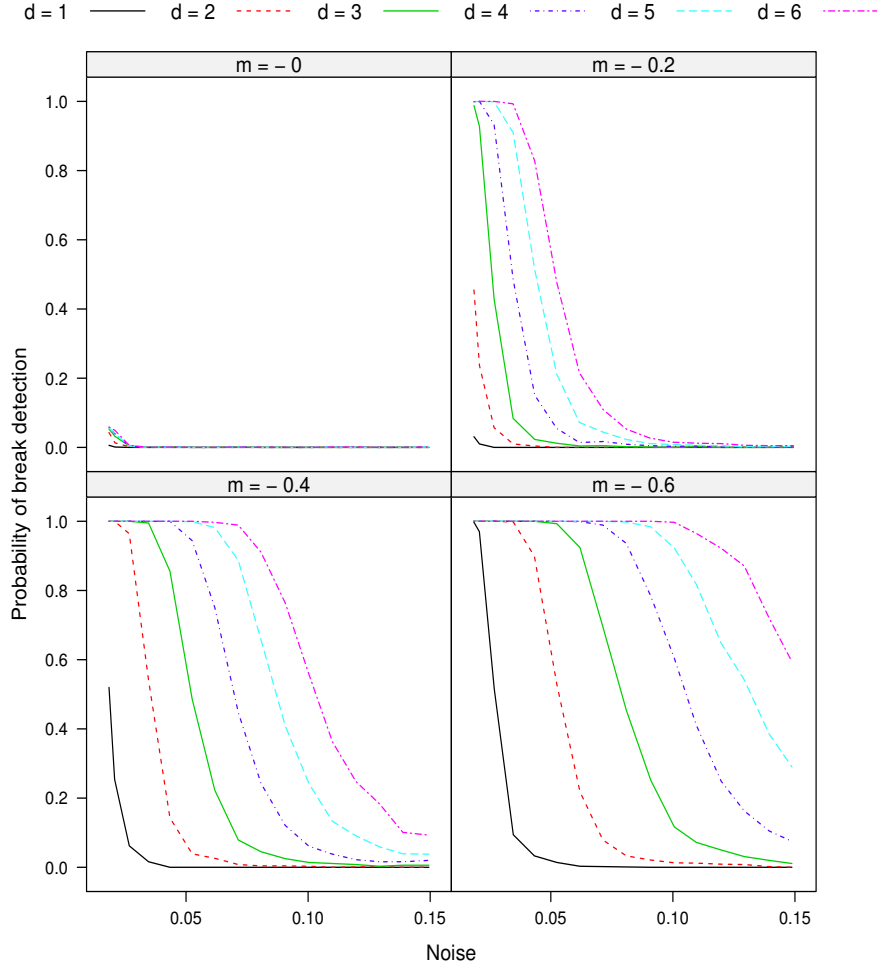
Figure 4: Results from the simulation experiment (1000 iterations) illustrating the probability of break detection in the monitoring period while varying the amount of noise (σ), magnitude of the simulated break (m), and amount of data available in the monitoring period (d). The units of the x- and y-axis are noise (i.e., σ NDVI of the residuals of the fitted season-trend model on the history period) and probability of detecting a break (i.e., proportion of detected breaks in 1000 iterations). See description of the simulation experiment for more details (Section 2.5).

influence the probability for break detection and results shown in Figure 4 are valid for the different simulated a's (Table 1). Random and NDVI-specific noise levels were introduced to simulate disturbances in the history period of the simulated time series and trigger identification of stable history periods with different lengths. The length of the identified stable history period did not influence the probability for break detection (results not shown). Furthermore, Figure 4 shows that a break with $m = -0.4$ can be detected when $\sigma < 0.1$ and $d \geq 3$. When the magnitude of the break is larger (e.g., $m = -0.6$), less observations ($d \geq 2$) are required for a similar amount of noise (e.g., $\sigma < 0.1$). Hence, Figure 4 illustrates that when $m = -0.6$, a $d = 4$ is needed for a greater than 60% chance of detecting the break when the noise level is $\sigma = 0.1$.

3.2. Drought disturbance detection in Somalia

We demonstrate the proof of concept of a multi-purpose near real-time disturbance detection method by analysing MODIS 16-day NDVI image time series. Here, the disturbance detection is limited to areas (1) with a minimum amount of vegetation cover by restricting the analysis to time series with a median NDVI > 0.2 during the 2000–2011 period (Vrieling *et al.* 2011) and (2) with a stable history longer than two years (see Section 3.1);

Figure 5a illustrates the median of an NDVI image time series (2000–2011) as a proxy for vegetation cover during the period of analysis. Areas with no or very low vegetation cover occur in North-Eastern Somalia whereas areas with higher vegetation cover are situated in the North-Western and Southern Somalia. Similar approaches have been used by Brown *et al.* (2010) and Vrieling *et al.* (2011) to study response of African land surface phenology. The NDVI time series with no or very low NDVI values are mainly influenced by irregular rainfall variations (results not shown). The areas with NDVI values above 0.2 in Figure 5a correspond to the areas where below normal rainfall and above normal land surface temperature is occurring (Figure 3) which illustrates that a severe drought is impacting areas with a minimum amount of vegetation cover (NDVI > 0.2).

Figure 5b illustrates the spatial variation of the length of the stable history period found by the ROC approach and used to restrict the disturbance monitoring (Figure 5d) to regions with a stable history longer than 2 years. The stable history is identified for modelling normal data variation within the history period to enable differentiation from abnormal changes, i.e., disturbances, in the monitoring period (i.e., mid-2010 onwards). The regions with a short stable history occurring in North-Eastern Somalia (Figure 5b) can be explained by the irregular and non-seasonal NDVI time series due a low vegetation cover (Figure 5a). The length of the stable history (Figure 5b) could also be used as an approximation of the occurrence of the most recent large disturbance in the history period (see Section 4 for discussion). The underlying NDVI time series for specific locations are shown in Figure 6 where for time series in Figures 6a and 6c the whole history period and in Figure 6b a shorter stable history period is identified as stable. Figure 6b shows that due to a drought-related disturbance in the NDVI time series at the beginning of 2008, not the full history period is used but a stable history period of 2.5 years is detected by the ROC approach.

Figure 5c shows the spatial variation of the noise level (i.e., $\hat{\sigma}$ of the residuals of the season-trend model) where low $\hat{\sigma}$ correspond to the low vegetated areas and the high $\hat{\sigma}$ correspond to the semi-arid ecosystems (e.g., woodland and savannah, see Figure 5a). High $\hat{\sigma}$ in the semi-arid ecosystems can be explained by large inter-annual phenological shifts (e.g., shifts in the start and end of the growing season) and double growing seasons when compared to areas with low vegetation cover or forested areas (Verbesselt *et al.* 2010b; Brown *et al.* 2010). Forest ecosystems when compared to semi-arid ecosystems (herbaceous land cover types) are more resistant to seasonal climate variations in rainfall and temperature due to the deeper rooting system (Verbesselt *et al.* 2006).

Figure 5c also illustrates that the noise range, 0–0.15, corresponds to the noise range of the simulation experiment (Figure 4) which confirms that the range of terrestrial ecosystem NDVI dynamics occurring in the study area were appropriately simulated for testing the proposed method in a controlled environment. The noise range shown in Figure 5c can be used when interpreting Figure 5d, since the simulation experiment (Figure 4) illustrated that σ is one of the main drivers of the probability to detect a disturbance. Figure 5d shows
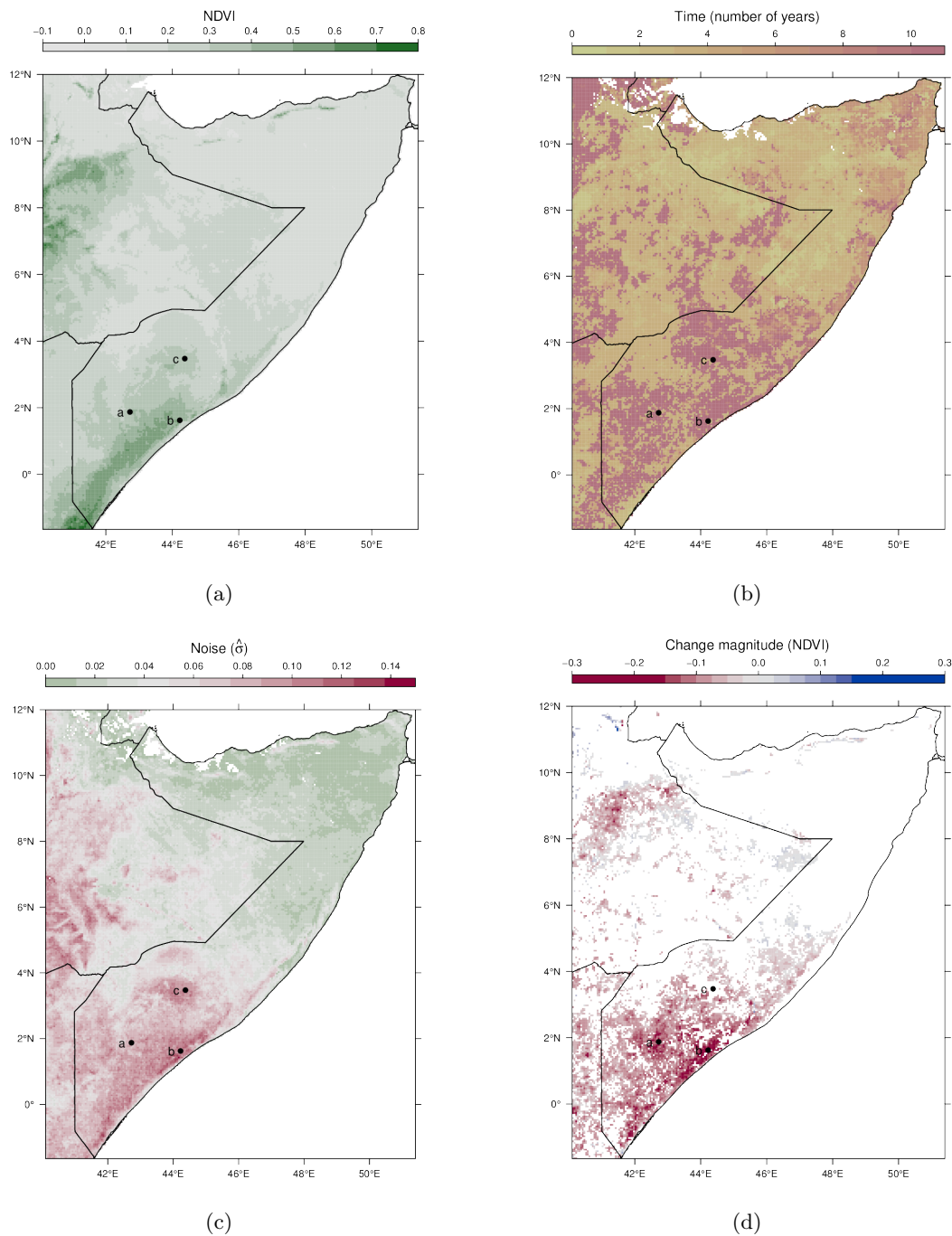
(a)

(b)

(c)

(d)

Figure 5: Results from the analysis of 16-day MODIS NDVI image time series from February 2000 until July 2011 covering Somalia; (a) median of all NDVI images as a proxy for vegetation cover during the 2000–2011 period, (b) length of the stable history period expressed in years where a shorter length is an indication of a more recent disturbance, (c) spatial variation of the noise level (i.e., the standard deviation of the residuals of the stable history model), (d) the change magnitude of the monitoring period containing a detected break (mid-2010 onwards) where white indicates that no disturbance is detected. The analysis of (d) was restricted to areas with minimum vegetation cover (i.e., median NDVI 2000–2011 > 0.2) and length of the history period > 2 years. Examples for three locations a, b, and c are shown in Figure 6.
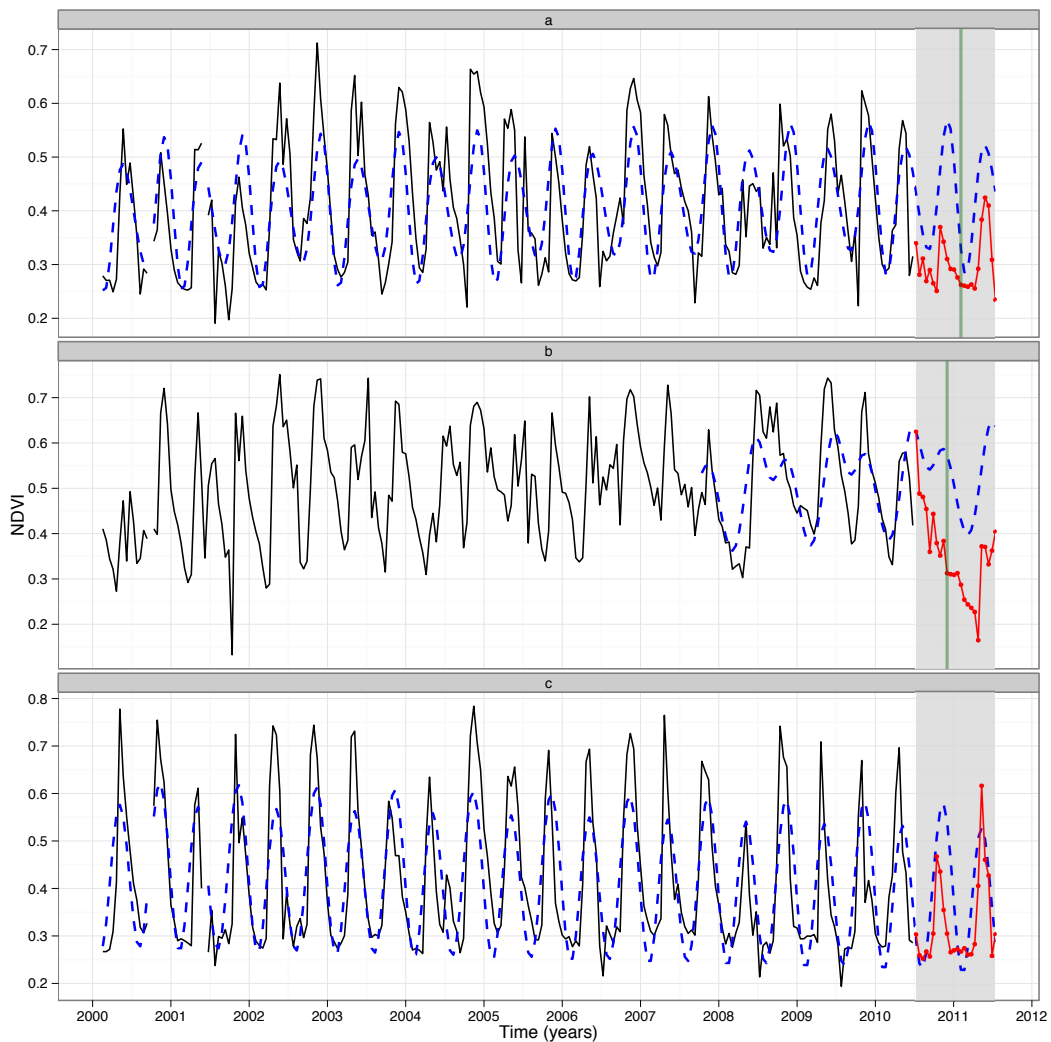
Figure 6: Results of real-time monitoring approach applied to 16-day MODIS NDVI time series for three locations a, b, and c shown in Figure 5. The period from 2000 until mid-2010, is considered the *history period* and the period from 2010 onwards is the *monitoring period* (grey background, red line). The stable history period within the history period (blue dashed line) is used to model and predict the normal data variation and enable disturbance detection in the monitoring period (Section 2.3). A disturbance is detected (green line) in Figures 6a and 6b after 14 and 10 observations, respectively.

the magnitude of the disturbance when detected in the monitoring period. Only disturbances with large negative magnitudes are detected and illustrate the effect of the 2010–2011 drought on vegetation photosynthetic capacity as measured by the NDVI in Somalia and surrounding countries (Funk 2011). Due to the high seasonal variability in the study area (i.e., high σ levels) only severe disturbances with large magnitude can be detected with the method, as illustrated in the simulation experiment (Figure 4). In summary, Figure 5d illustrates the severity of the ongoing drought and corresponds with the regions in South Somalia showing most intense drought anomaly (Figure 3).

Figure 6a and b illustrate two examples of NDVI time series where a disturbance with a negative magnitude is detected in the monitoring period. The negative magnitude is clearly shown by the lack of seasonality and major decrease in NDVI from mid-2010 onwards. Statistically significant disturbances are detected from mid-July 2010 onwards and illustrate capacity of the proposed multi-purpose disturbance detection method.

4. Discussion

Real-time satellite images and anomaly products are routinely produced (e.g., `http://www.fews.net/`) but can be further improved by using the full temporal detail of the satellite image time series. Here, we propose a time series analysis approach that automatically identifies a stable *history period* within time series to model normal expected behaviour and enables detection of abnormal events (i.e., disturbances) within new observations (i.e., *monitoring period*). Current operational food security monitoring by organisations as FEWS-NET, JRC, and FAO concentrate on mapping of NDVI anomalies deviating from a long-term mean. Anomalies compared to a mean do not take into account gradual and seasonal variability (Vrieling *et al.* 2011). The method proposed here addresses this issue and models normal season-trend variation (Equation 1) of an automatically identified stable history period to enable drought disturbance detection in the monitoring period.

The method is tested in a controlled environment by simulating time series containing disturbances and demonstrated by applying it to 16-day MODIS NDVI image time series covering Somalia to assess the significance of the drought impact on the vegetation dynamics. NDVI time series representing a wide range of terrestrial ecosystems are simulated and results illustrate that when more than two new observations are available in the *monitoring* period disturbance detection becomes possible. However, simulation results also showed that the noise level remaining after fitting the season-trend model is the main driver of the capacity to quickly detect disturbances and as such also highlights the limitations of the method. Due to the fact that the approach is a data-driven method, the signal-to-noise ratio determines the capacity of the method to differentiate between change and no-change. Hence, a disturbance can be detected when the signal of the disturbance is significantly different from the signal-to-noise ratio of the modelled history period. For example, the simulation results indicate that at $m = -0.4$, in order to identify the break with a probability of 60%, three observations ($d = 3$) are required while the noise level would need to be less than 0.05. In the real-world example a magnitude of -0.4 is not reached and noise levels are higher than 0.05 for the areas of interest a, b, and c in Figure 5c. Hence, the comparison of the real world case study with the simulation results shows that more than two observation (i.e., $d > 2$) are needed to be able to detect a disturbance with a probability larger than 60% since noise levels in the areas of interest are higher (Figure 6). This example illustrates besides the limitations of the monitoring method also the importance of combining the results of the simulation and real world example. However, the comparison between simulation and real-world data is based on some assumptions: (1) that the type of simulated disturbance (i.e., a step change in this study) corresponds to the disturbances occurring in the real-world example, (2) that the change magnitude of the simulated data (i.e., vertical difference of the step change) can be compared with the estimated magnitude of the real-world example (i.e., the difference between the estimated season-trend model and the actual data in the monitoring period). These assumptions highlight the care that should be taken when comparing simulation and real-world results.

Further work is needed to evaluate the capacity of the proposed method to reliably detect disturbances (i.e., probability to detect a change) within a reasonable amount of time (i.e., amount of data needed) for different data series and change types (e.g., deforestation).

We can conclude that the signal-to-noise ratio is driving the change detection capacity and that consequently the data preprocessing in order to improve the quality and reliability of time series data remains essential to improve disturbance detection. Furthermore, the real-world example shows that major disturbances are detected in Southern Somalia from mid-July 2010 onwards and illustrates the severity of the drought affecting the photosynthetic capacity of the vegetation. As such, the proof of concept of the method as a near real-time disturbance detection system that can be integrated within existing early warning systems for automated disturbance detection (e.g., drought or deforestation). Three items can be further discussed in detail.

(1) Results confirm the importance of a simulation experiment when developing change detection methods. Novel methods can be tested in a controlled environment while varying individual parameters. When detecting changes in real data at a global scale often accurate field data about disturbances and influencing factors (e.g., quality of the time series observations) are not available. However, it is challenging to create simulated time series that approximate remotely sensed time series (Zhang *et al.* 2009). For example, it is important to assess the effect of inter-yearly seasonal shifts in real satellite data (e.g., shifts in the growing season) as these can increase the noise level σ and reduce the probability of disturbance detection. The inter-yearly seasonal variation is especially high in grasslands, savannah regions with a high herbaceous cover fraction and unpredictable rainfall (de Jong *et al.* 2011). The effect of inter-yearly seasonal variations has been simulated in this experiment by introducing high σ levels (i.e., up to $\sigma = 0.15$, Table 1). The empirical noise levels $\hat{\sigma}$ remaining after fitting the season-trend model on the stable history period of the MODIS image time series data shown in Figure 5c confirms that the range of NDVI dynamics occurring in the study area were appropriately simulated for testing the proposed method.

(2) The accuracy of estimating the time of disturbance was not assessed in the simulation experiment. The proposed method is developed as a fast, multi-purpose and globally applicable alert system for disturbances within newly acquired data of available time series observations. Also, in the real-world case study the objective was to assess whether the ongoing drought had a significant effect on the vegetation dynamics and not to assess the precise timing of the disturbance within the monitoring period. In previous work, the BFAST method was proposed to determine the number, type, and timing of trend and seasonal changes within historical time series (Verbesselt *et al.* 2010a) whereas, here, we focussed on disturbance detection in newly acquired observations. A possible operational workflow for disturbance monitoring could be to (a) verify whether or not a disturbance is occurring in new observations using the method proposed here and then (b) if a disturbance is detected the timing, magnitude and direction of change can be determined when more data is available.

Similarly, the accuracy of the estimated stable history length was not assessed. The ROC approach (Pesaran and Timmermann 2002) was used here as an automated approach to identify a stable history period without disturbances and is not developed for accurate time estimation of disturbances in the history period. The ROC approach (Section 2.4)

verifies whether or not a structural change is occurring while stepwise going back in history. If a more precise estimate of the timing of the last major prior disturbance is of interest, more appropriate methods are available, e.g., Bai and Perron (2003), adapted in Verbesselt *et al.* (2010a). There are two alternatives for determining the stable history period. First, the BFAST approach can be used for a more accurate estimation of disturbances in the history period and can help identify a stable history period within a time series. However, BFAST is computationally more expensive than the ROC method for determining the stable history due to the iterative locally optimal time-of-break estimation. Second, as previously pointed out, expert knowledge can be utilised to select the stable history period manually for a specific area of interest, but at regional or global scale this is typically hard to obtain and implement. This functionality is available in the real-time monitoring function in the *bfast* package for R (R Development Core Team 2011). Furthermore, we recommend limiting the disturbance detection to time series with a sufficiently stable history period to enable a reliable estimation of the 8 season-trend model parameters (Equation 1), e.g., longer than 2 years in this study corresponding to 46 observations of 16-day data.

(3) BFAST, like most other change detection methods, does not directly provide interpretive information about the source of the disturbance (e.g., a disturbance within a NDVI time series). However, the detected disturbances within NDVI time series in South East Somalia can be explained by the lack of rainfall (Figure 3). Moreover, previous research has illustrated that the NDVI time series are closely related to the rainfall dynamics in water limited ecosystems and can be used for drought detection and prediction (Funk and Budde 2009; Vrieling *et al.* 2011).

While the data and methods used are appropriate for proof-of-concept development of global scale disturbance monitoring, specific applications (e.g., drought or deforestation monitoring) mandates integration within an operational early warning framework (e.g., `http://www.fews.net/` or `http://earlywarning.usgs.gov/`). For example, the lack of rainfall can explain why a harvest fails but it often is not the only factor explaining the food security problem in a country. Also factors such as poverty, market forces, conflict, lack of infrastructure, and HIV/AIDS play an important role (Funk 2011; Vrieling *et al.* 2011). Still, analysis of climate and NDVI variability provides important input for food security analysis and further work is required to assess how the real-time disturbance detection approach can be implemented in an operational framework or as an independent alert system in other regions in the world where real-time monitoring systems are not implemented yet (Asner 2011).

5. Conclusion

The paper introduces a multi-purpose near real-time disturbance monitoring approach based on a BFAST-type season-trend model, that is applicable to different types of time series (e.g., in-situ or satellite sensors). The BFAST monitoring method analyses time series and automatically identifies and models the stable history part of a time series in order to detect disturbances within newly acquired data. The method can be applied to time series to enable a rapid response by detecting disturbances in near real-time. BFAST monitoring has the following characteristics that make it appropriate for near real-time global scale disturbance detection: It (1) is fast and requires a minimum amount of processing time (e.g., 0.02 seconds

to analyse one pixel of 10 year-long 16-day time series on a normal desktop computer), (2) does not require the definition of thresholds, (3) can analyse time series with data gaps (e.g., masked clouds or sensor defects) and does not require gap filling techniques, and (4) analyses the full temporal detail of a time series. This is of particular importance since robust methods for analysis of satellite image time series are critically needed as longer high temporal and spatially detailed image time series are becoming available. For example, with the advent of novel satellite sensors, like the European Space Agency Sentinel satellite constellation, time-series-based disturbance detection will become possible at more detailed spatial scales where many human-induced change processes operate. Furthermore, the real-time monitoring method is implemented in open-source software environment and is freely available in the *bfast* package for R (R Development Core Team 2011). More information illustrating how to apply the method on satellite image time series are available at `http://bfast.R-Forge.R-project.org/` and the example section of the *bfastmonitor()* function within the *bfast* package.

Acknowledgments

References

Acker JG, Leptoukh G (2007). "Online Analysis Enhances use of NASA Earth Science Data." *EOS*, **88**(2), 14–17.

Asner GP (2011). "Painting the World REDD: Addressing Scientific Barriers to Monitoring Emissions from Tropical Forests." *Environmental Research Letters*, **6**(2), 021002.

Bai J, Perron P (2003). "Computation and Analysis of Multiple Structural Change Models." *Journal of Applied Econometrics*, **18**(1), 1–22.

Brown ME, de Beurs KM, Vrieling A (2010). "The Response of African Land Surface Phenology to Large Scale Climate Oscillations." *Remote Sensing of Environment*, **114**(10), 2286–2296.

Chu CSJ, Stinchcombe M, White H (1996). "Monitoring Structural Change." *Econometrica*, **64**(5), 1045–1065.

Cryer JD, Chan KS (2008). *Time Series Analysis – With Applications in R.* 2nd edition. Springer-Verlag, New York.

de Beurs KM, Henebry GM (2005). "Land Surface Phenology and Temperature Variation in the International Geosphere-Biosphere Program High-Latitude Transects." *Global Change Biology*, **11**(5), 779–790.

de Beurs KM, Wright CK, Henebry GM (2009). "Dual Scale Trend Analysis for Evaluating Climatic and Anthropogenic Effects on the Vegetated Land Surface in Russia and Kazakhstan." *Environmental Research Letters*, **4**(4).

de Jong R, Verbesselt J, Schaepman ME, de Bruin S (2011). "Trend Changes in Global Greening and Browning: Contribution of Short-Term Trends to Longer-Term Change." *Global Change Biology*, **18**(2), 1–15.

Funk C (2011). "We Thought Trouble Was Coming." *Nature*, **476**(7358), 7.

Funk C, Budde ME (2009). "Phenologically-Tuned MODIS NDVI-Based Production Anomaly Estimates for Zimbabwe." *Remote Sensing of Environment*, **113**(1), 115–125.

Geerken RA (2009). "An Algorithm to Classify and Monitor Seasonal Variations in Vegetation Phenologies and Their Inter-Annual Change." *ISPRS Journal of Photogrammetry and Remote Sensing*, **64**(4), 422–431.

Hargrove WW, Spruce JP, Gasser GE, Hoffman FM (2009). "Toward a National Early Warning System for Forest Disturbances Using Remotely Sensed Canopy Phenalogy." *Photogrammetric Engineering and Remote Sensing*, **75**(10), 1150–1156.

Hayes DJ, Cohen WB (2007). "Spatial, Spectral and Temporal Patterns of Tropical Forest Cover Change as Observed with Multiple Scales of Optical Satellite Data." *Remote Sensing of Environment*, **106**(1), 1–16.

Huete A, Didan K, Miura T, Rodriguez EP, Gao X, Ferreira LG (2002). "Overview of the Radiometric and Biophysical Performance of the MODIS Vegetation Indices." *Remote Sensing of Environment*, **83**(1-2), 195–213.

Jiang L, Kogan FN, Guo W, Tarpley JD, Mitchell KE, Ek MB, Tian Y, Zheng W, Zou CZ, Ramsay BH (2010). "Real-Time Weekly Global Green Vegetation Fraction Derived from Advanced Very High Resolution Radiometer-Based NOAA Operational Global Vegetation Index (GVI) System." *Journal Of Geophysical Research-Biogeosciences*, **115**(D11114).

Jin SM, Sader SA (2005). "MODIS Time-Series Imagery for Forest Disturbance Detection and Quantification of Patch Size Effects." *Remote Sensing of Environment*, **99**(4), 462–470.

Jönsson P, Eklundh L (2002). "Seasonality Extraction by Function Fitting to Time-Series of Satellite Sensor Data." *IEEE Transactions on Geoscience and Remote Sensing*, **40**(8), 1824–1832.

Julien Y, Sobrino JA (2010). "Comparison of Cloud-Reconstruction Methods for Time Series of Composite NDVI Data." *Remote Sensing of Environment*, **114**(3), 618–625.

Kennedy RE, Cohen WB, Schroeder TA (2007). "Trajectory-Based Change Detection for Automated Characterization of Forest Disturbance Dynamics." *Remote Sensing of Environment*, **110**(3), 370–386.

Leisch F, Hornik K, Kuan CM (2000). "Monitoring Structural Changes with the Generalized Fluctuation Test." *Econometric Theory*, **16**, 835–854.

Lu D, Mausel P, Brondizio E, Moran E (2004). "Change Detection Techniques." *International Journal of Remote Sensing*, **25**(12), 2365–2407.

Muchiri PW (2007). "Climate of Somalia." *Technical report W-01*, Somalia Water and Land Information Management (SWALIM), Nairobi, Kenya.

Myneni RB, Hall FG, Sellers PJ, Marshak AL (1995). "The Interpretation of Spectral Vegetation Indexes." *IEEE Transactions on Geoscience and Remote Sensing*, **33**(2), 481–486.

Myneni RB, Keeling CD, Tucker CJ, Asrar G, Nemani RR (1997). "Increased Plant Growth in the Northern High Latitudes from 1981 to 1991." *Nature*, **386**(6626), 698–702.

Pesaran MH, Timmermann A (2002). "Market Timing and Return Prediction under Model Instability." *Journal of Empirical Finance*, **9**, 495–510.

Pettorelli N, Vik JO, Mysterud A, Gaillard JM, Tucker CJ, Stenseth NC (2005). "Using the Satellite-Derived NDVI to Assess Ecological Responses to Environmental Change." *Trends in Ecology and Evolution*, **20**(9), 503–510.

Pickett STA, White PS (1986). "An Introduction." In *The Ecology of Natural Disturbance and Patch Dynamics*, pp. 3–13. Academic Press, New York.

Potter C, Tan PN, Steinbach M, Klooster S, Kumar V, Myneni R, Genovese V (2003). "Major Disturbance Events in Terrestrial Ecosystems Detected Using Global Satellite Data Sets." *Global Change Biology*, **9**(7), 1005–1021.

R Development Core Team (2011). *R: A Language and Environment for Statistical Computing*. R Foundation for Statistical Computing, Vienna, Austria. URL http://www.R-project.org/.

Roerink GJ, Menenti M, Verhoef W (2000). "Reconstructing Cloudfree NDVI Composites Using Fourier Analysis of Time Series." *International Journal of Remote Sensing*, **21**(9), 1911–1917.

Rojas O, Rembold F, Royer A, Negre T (2005). "Real-Time Agrometeorological Crop Yield Monitoring in Eastern Africa." *Agronomy for Sustainable Development*, **25**(1), 63–77.

Roy DP, Borak JS, Devadiga S, Wolfe RE, Zheng M, Descloitres J (2002). "The MODIS Land Product Quality Assessment Approach." *Remote Sensing of Environment*, **83**(1-2), 62–76.

Samanta A, Costa MH, Nunes EL, Vieira SA, Xu L, Myneni RB (2011). "Comment on "Drought-Induced Reduction in Global Terrestrial Net Primary Production from 2000 through 2009"." *Science*, **333**(6046), 1093–1093.

Schimel DS, House JI, Hibbard KA, Bousquet P, Ciais P, Peylin P, Braswell BH, Apps MJ, Baker D, Bondeau A, Canadell J, Churkina G, Cramer W, Denning AS, Field CB, Friedlingstein P, Goodale C, Heimann M, Houghton RA, Melillo JM, Moore III B, Murdiyarso D, Noble I, Pacala SW, Prentice IC, Raupach MR, Rayner PJ, Scholes RJ, Steffen WL, Wirth C (2001). "Recent Patterns and Mechanisms of Carbon Exchange by Terrestrial Ecosystems." *Nature*, **414**(6860), 169–172.

Stone C, Turner R, Verbesselt J (2008). "Integrating Plantation Health Surveillance and Wood Resource Inventory Systems Using Remote Sensing." *Australian Forestry*, **71**(3), 245–253.

Turner MG (2010). "Disturbance and Landscape Dynamics in a Changing World." *Ecology*, **91**(10), 2833–2849.

Verbesselt J, Hyndman R, Newnham G, Culvenor D (2010a). "Detecting Trend and Seasonal Changes in Satellite Image Time Series." *Remote Sensing of Environment*, **114**(1), 106–115.

Verbesselt J, Hyndman R, Zeileis A, Culvenor D (2010b). "Phenological Change Detection while Accounting for Abrupt and Gradual Trends in Satellite Image Time Series." *Remote Sensing of Environment*, **114**(12), 2970–2980.

Verbesselt J, Jönsson P, Lhermitte S, van Aardt J, Coppin P (2006). "Evaluating Satellite and Climate Data Derived Indices as Fire Risk Indicators in Savanna Ecosystems." *IEEE Transactions on Geoscience and Remote Sensing*, **44**(6), 1622–1632.

Verbesselt J, Robinson A, Stone C, Culvenor D (2009). "Forecasting Tree Mortality Using Change Metrics Derived from MODIS Satellite Data." *Forest Ecology and Management*, **258**(7), 1166–1173.

Verdin J, Funk C, Senay G, Choularton R (2005). "Climate Science and Famine Early Warning." *Philosophical Transactions of the Royal Society B*, **360**(1463), 2155–2168.

Vogelmann JE, Xian G, Homer C, Tolk B (2012). "Monitoring Gradual Ecosystem Change Using Landsat Time Series Analyses: Case Studies in Selected Forest and Rangeland Ecosystems." *Remote Sensing Of Environment*, pp. 1–14.

Vrieling A, de Beurs KM, Brown ME (2011). "Variability of African Farming Systems from Phenological Analysis of NDVI Time Series." *Climatic Change*, pp. 1–23.

White MA, de Beurs KM, Didan K, Inouye DW, Richardson AD, Jensen OP, O'Keefe J, Zhang G, Nemani RR, van Leeuwen WJD, Brown JF, de Wit A, Schaepman M, Lin X, Dettinger M, Bailey AS, Kimball J, Schwartz MD, Baldocchi DD, Lee JT, Lauenroth WK (2009). "Intercomparison, Interpretation, and Assessment of Spring Phenology in North America Estimated from Remote Sensing for 1982–2006." *Global Change Biology*, **15**, 2335–2359.

White MA, Nemani RR (2006). "Real-Time Monitoring and Short-Term Forecasting of Land Surface Phenology." *Remote Sensing of Environment*, **104**(1), 43–49.

Wolfe RE, Roy DP, Vermote E (1998). "MODIS Land Data Storage, Gridding, and Compositing ethodology: Level 2 Grid." *IEEE Transactions on Geoscience and Remote Sensing*, **36**(4), 1324–1338.

Xie PP, Arkin PA (1997). "Global Precipitation: A 17-Year Monthly Analysis Based on Gauge Observations, Satellite Estimates, and Numerical Model Outputs." *Bulletin of the American Meteorological Society*, **78**(11), 2539–2558.

Zeileis A (2005). "A Unified Approach to Structural Change Tests Based on ML Scores, *F* Statistics, and OLS Residuals." *Econometric Reviews*, **24**(4), 445–466.

Zeileis A, Leisch F, Hornik K, Kleiber C (2002). "strucchange: An R Package for Testing for Structural Change in Linear Regression Models." *Journal of Statistical Software*, **7**(2), 1–38.

Zeileis A, Leisch F, Kleiber C, Hornik K (2005). "Monitoring Structural Change in Dynamic Econometric Models." *Journal of Applied Econometrics*, **20**(1), 99–121.

Zeileis A, Shah A, Patnaik I (2010). "Testing, Monitoring, and Dating Structural Changes in Exchange Rate Regimes." *Computational Statistics & Data Analysis*, **54**(6), 1696–1706.

Zhang XY, Friedl MA, Schaaf CB (2009). "Sensitivity of Vegetation Phenology Detection to the Temporal Resolution of Satellite Data." *International Journal of Remote Sensing*, **30**(8), 2061–2074.

Affiliation:

Jan Verbesselt, Martin Herold
Remote sensing team
Wageningen University
Droevendaalsesteeg 3
Wageningen 6708 PB, The Netherlands
E-mail: Jan.Verbesselt@wur.nl, Martin.Herold@wur.nl
URL: http://www.grs.wur.nl/

Achim Zeileis
Department of Statistics
Universität Innsbruck
Universitätsstr. 15
6020 Innsbruck, Austria
E-mail: Achim.Zeileis@R-project.org
URL: http://eeecon.uibk.ac.at/~zeileis/